

Nitrification in the Euphotic Zone as a Source for Nitrite, Nitrate, and Nitrous Oxide at Station ALOHA

John E. Dore; David M. Karl

Limnology and Oceanography, Vol. 41, No. 8 (Dec., 1996), 1619-1628.

Stable URL:
http://links.jstor.org/sici?sici=0024-3590%28199612%2941%3A8%3C1619%3ANITEZA%3E2.0.CO%3B2-8

Limnology and Oceanography is currently published by American Society of Limnology and Oceanography.

Your use of the JSTOR archive indicates your acceptance of JSTOR's Terms and Conditions of Use, available at http://www.jstor.org/about/terms.html. JSTOR's Terms and Conditions of Use provides, in part, that unless you have obtained prior permission, you may not download an entire issue of a journal or multiple copies of articles, and you may use content in the JSTOR archive only for your personal, non-commercial use.

Please contact the publisher regarding any further use of this work. Publisher contact information may be obtained at http://www.jstor.org/journals/limnoc.html.

Each copy of any part of a JSTOR transmission must contain the same copyright notice that appears on the screen or printed page of such transmission.

JSTOR is an independent not-for-profit organization dedicated to creating and preserving a digital archive of scholarly journals. For more information regarding JSTOR, please contact support@jstor.org.

http://www.jstor.org/
Thu Mar 10 15:02:28 2005

Limnol. Oceanogr., 41(8), 1996, 1619–1628
© 1996, by the American Society of Limnology and Oceanography, Inc.

Nitrification in the euphotic zone as a source for nitrite, nitrate, and nitrous oxide at Station ALOHA

John E. Dore and David M. Karl
Department of Oceanography, School of Ocean and Earth Science and Technology, University of Hawaii, Honolulu 96822

Abstract

We measured chemoautotrophic bacterial nitrification rates in the lower euphotic zone at the North Pacific Time-series Station ALOHA using low-level chemical assays and inhibitor-sensitive radiocarbon uptake experiments. These measurements were compared with independent nitrification rate estimates based on nitrous oxide distributions, nitrate assimilation rates based on nitrate changes during an in situ incubation, and historical estimates of nitrification and nitrate assimilation from this region. Ammonium oxidation rates ranged from 1.0 to 137.4 μmol m^{-3} d^{-1}, and nitrite oxidation rates varied from undetectable to 138.0 μmol m^{-3} d^{-1}. Conservative estimates of depth-integrated euphotic zone nitrification rates from the complete three-cruise data set were 0.69 mmol m^{-2} d^{-1} for nitrite oxidation and 1.64 mmol m^{-2} d^{-1} for ammonium oxidation. The highest nitrification rates were found below the primary nitrite maximum, suggesting a significant contribution of euphotic zone ammonium oxidation to the nitrite pool below but not within this feature. A mass balance of nitrous oxide indicates that this gas is produced within the euphotic zone at a rate of 1.68–7.94 μmol m^{-2} d^{-1}. The nitrous oxide production rate provides an independent estimate of the total euphotic zone nitrification rate in the range of 0.34–1.59 mmol m^{-2} d^{-1}. We estimate that the total euphotic zone nitrification rate is 47–142% of the concurrent nitrate assimilation rate, indicating that nitrification in the euphotic zone is an important source of regenerated nitrate.

Nitrification, the microbiologically mediated oxidation of ammonium to nitrite and nitrite to nitrate, is a key process in the global nitrogen cycle (Ward 1986). In the marine environment, the vertical flux into the euphotic zone of nitrate regenerated by nitrification in deep water is considered crucial to ecosystem stability through its support of new primary photosynthetic production (Eppley and Peterson 1979). However, nitrifying bacteria are also active within the euphotic zone, especially within the primary nitrite maximum (Olson 1981*a*; Ward et al. 1982). Although primary production based on nitrate is usually equated with new production (Dugdale and Goering 1967; Eppley and Peterson 1979), if the nitrate is produced within the euphotic zone, it must be considered recycled production. Consequently, if nitrification in an oceanic ecosystem proceeds at a substantial rate within the euphotic zone, then nitrate uptake cannot be equated with new production for that ecosystem (Dugdale and Goering 1967; Priscu and Downes 1985; Ward et al. 1989).

It has been suggested that bacterial nitrification is responsible for the maintenance of the primary nitrite maximum (PNM), an accumulation of nitrite found in the lower euphotic zone over much of the world's oceans (Rakestraw 1936; Brandhorst 1959; Olson 1981*b*). However, the excretion of nitrite by phytoplankton during nitrate assimilation has also been implicated as a nitrite source (Vaccaro and Ryther 1960; Kiefer et al. 1976; Herbland and Voituriez 1979). At oligotrophic oceanic sites such as the Hawaii Ocean Time-series Station ALOHA (22°45′N, 158°W), the PNM is located well within the euphotic zone (Dore and Karl 1996). Knowledge of the relative importance of these oxidative and reductive processes is therefore necessary for an accurate understanding of the nitrogen cycle in such areas.

Furthermore, nitrification produces the ozone-depleting greenhouse gas nitrous oxide as a metabolic by-product (Ritchie and Nicholas 1972). Euphotic zone nitrification represents a near-surface source of this trace gas (Capone 1991), yet other processes potentially contribute to the generation of nitrous oxide within the euphotic zone as well (Kaplan and Wofsy 1985).

The distribution and magnitude of euphotic zone nitrification processes are clearly important factors to consider in biogeochemical studies of marine primary production as well as nitrogen and carbon cycling. We report here the results of a number of field observations and rate experiments designed to elucidate the extent of euphotic zone nitrification and its potential influence on recycled production, the sea-air flux of nitrous oxide, and the distribution of nitrite at Station ALOHA.

Materials and methods

All sampling and experiments were performed at Station ALOHA (A Long-term Oligotrophic Habitat Assessment), a North Pacific deep water (>4,500 m) site visited at approximately monthly intervals as part of the

Acknowledgments

We thank the Hawaii Ocean Time-series personnel, especially R. Letelier, D. Hebel, C. Carrillo, L. Tupas, C. Winn, and R. Lukas, as well as the captains and crews of the RV *Moana Wave, Thomas G. Thompson,* and *Wecoma* for professional assistance. J. Priscu, F. Sansone, and C. Measures provided technical advice on the analysis of nitrous oxide in seawater.

Financial support was provided by National Science Foundation grants OCE 87-17195 (R. Lukas, P.I.), OCE 88-00329 (D.M.K.), and OCE 93-01368 (D.M.K.) and by a fellowship from the Research Corporation of the University of Hawaii awarded to J.E.D. This is SOEST contribution 4114 and U.S.-JGOFS contribution 231.

Hawaii Ocean Time-series (HOT) project (Karl and Lukas 1996). The oligotrophic waters at Station ALOHA are considered representative of the North Pacific subtropical gyre. Sampling is restricted to a circle with an 11-km radius centered at 22°45′N, 158°W, 100 km north of Kahuku Point, Oahu, Hawaii.

A CTD/rosette system equipped with 24 12-liter PVC bottles with Teflon-coated springs was used for sample collection. The protocols for CTD operation, data analysis, and sensor calibration are described elsewhere (Bingham and Lukas 1996). The surface flux of photosynthetically available radiation (PAR; 400–700 nm) was measured with a LiCor cosine collector. Underwater PAR was determined with a hand-lowered Biospherical profiling natural fluorometer.

The depth of the euphotic zone, defined here as the phytoplankton compensation depth (Sverdrup 1953), can be estimated as the depth at which inorganic carbon incorporation in the light is not significantly ($P \leq 0.05$) greater than in the dark, assuming that total community respiration is the same in the light as in the dark. This depth has been found to be 173±7 m at Station ALOHA (Letelier et al. 1996); for convenience, we will assume this depth is 175 m throughout this paper. The PAR at this depth is 0.05% (±0.01%) of the surface PAR flux (Letelier et al. 1996).

Nitrite and nitrate—Water samples for nitrite (NO_2^-) and nitrate (NO_3^-) were drawn with clean Tygon tubing into acid-washed 125-ml polyethylene bottles and stored frozen as described by Dore and Karl (1996) for later analysis at our shore-based laboratory. Concentrations of nitrite and of the sum of nitrate and nitrite (N+N) were measured by the chemiluminescent methods developed by Cox (1980) and Garside (1982), which offer detection limits and precisions of 2 μmol m^{-3} or less (Dore and Karl 1996). Nitrate was calculated by difference. Even when these low-level methods have been used, no significant effect of the sample preservation and storage by freezing has been noted for NO_2^- (Dore and Karl 1996) or for N+N (Dore et al. 1996). In all nitrification rate experiments, both NO_2^- and N+N were determined on the same samples, but the water column profiles of N+N were determined on separate casts; therefore, water column NO_3^- is not reported separately. In these cases, the NO_2^- and N+N sample depths are aligned by means of potential densities. This alignment is performed so that the relative positions of features are not altered by short-term internal wave motions, which have been shown to vertically displace isopycnals at Station ALOHA by 10s of meters in a few hours (Dore and Karl 1996).

Nitrous oxide—Samples for nitrous oxide (N_2O) were collected in 250-ml glass BOD-type bottles with ground-glass stoppers. Clean Tygon tubing was used to rinse and fill each sample bottle from the bottom, allowing at least two volumes of sample to overflow in the process and to displace all bubbles. Each sample was then aspirated to just below the neck, poisoned with 100 μl of saturated mercuric chloride, and its stopper was replaced after light lubrication with a carbon-based grease (Apiezon) to prevent gas exchange during storage. The stoppers were secured with polyethylene tape, and the samples were stored in the dark at laboratory temperature (~20°C) until the day of analysis. Nitrous oxide samples stored in a similar manner have been demonstrated to be stable for at least 1.5 months (Elkins 1980; Butler and Elkins 1991). Although the storage time for our samples ranged from a few days to several months, we found no trend in the relationship between measured N_2O concentration and storage time.

Nitrous oxide analysis was achieved by the equilibration of a subsample with an ultra-pure helium headspace in a gas-tight syringe, followed by analysis of the headspace with a gas chromatograph (Varian model 3300) outfitted with a ^{63}Ni electron capture detector held at 360°C. The protocol was similar to that of Elkins (1980), except that our instrument was configured for backflushing to prevent interference from water-associated halocarbons, and we did not use multiple equilibrations. Separation was achieved on a 3-m column packed with Chromosorb 102 (80/100 mesh) and kept at 55°C. The carrier gas was an ultra-high purity 5% mixture of methane in argon; ultra-high purity helium was used for sample equilibrations and backflushing. Both gases were further purified with molecular sieve 5A and an oxygen scrubber.

Nitrous oxide concentration and percent saturation were calculated by means of published equations for seawater (Weiss and Price 1980) and assuming an atmospheric mixing ratio of 312 ppbv. We have assumed this mixing ratio based on the world mean tropospheric N_2O concentration in 1990 (310 ppbv) extrapolated to 1993 by assuming a yearly rise of 0.25% (Houghton et al. 1990). Because of the questionable absolute accuracy of commercially available standard N_2O mixtures (Rasmussen and Pierotti 1978), we normalized our working standards to this mixing ratio for air and used clean air from upwind of Oahu as a primary standard. The response of our instrument to such air samples varied by no more than 1% over a period of several months. The average precision of the seawater N_2O assay, based on 14 samples that were collected and stored in duplicate, was ±3.4%.

Nitrification and nitrate uptake rates—Chemoautotrophic ammonium oxidation rates were determined by an inhibitor-sensitive dark radiocarbon (^{14}C) uptake assay (Billen 1976; Somville 1978) and independently by a chemical assay. Chemoautotrophic nitrite oxidation rates were also measured with a chemical assay. During one cruise (HOT-31), we used both methods simultaneously to check the validity of the conversion factors chosen for the ^{14}C-based method.

The ^{14}C-based assay relies upon measurement of the dark incorporation of $H^{14}CO_3^-$ into particulate organic matter within an incubated water sample with and without the addition of a metabolic inhibitor that is known to affect ammonium oxidizing bacteria. Incubations were conducted in the dark to prevent interference from photoautotrophic carbon assimilation and were temperature controlled to simulate in situ conditions. The difference

between the ^{14}C assimilated in the controls and that assimilated in the inhibited samples is a measure of the growth of ammonium oxidizing bacteria.

We used acetylene gas (C_2H_2) as an inhibitor of ammonium oxidation. Acetylene is known to be an effective inhibitor of ammonium oxidation (Hynes and Knowles 1981) and is highly water soluble. Acetylene also inhibits denitrification, but because denitrification is not an autotrophic process, its inhibition should not appreciably affect the results of the ^{14}C-based assay. Nitrapyrin (N-Serve; Dow Chemical) is more commonly used as a nitrification inhibitor; however, it has been noted that in oligotrophic oceanic waters, nitrapyrin can act as a general metabolic inhibitor (Ward 1986). Nitrapyrin also must be introduced dissolved in a solvent, which itself can affect metabolism (Ward 1986), whereas acetylene is introduced as a highly purified gas.

On each cruise, a nighttime rosette cast was made to collect samples from up to 24 depths within the upper 200 m. Nitrification rate experiments were conducted on water from two to four depths within the 100–175-m depth range. We focused on this depth range because previous studies have indicated that given the water clarity at Station ALOHA, nitrifiers from water shallower than 100 m should be nearly completely photoinhibited (Olson 1981*b*; Dore and Karl 1996). Water samples (400 ml) were collected directly from the rosette bottles under subdued light into acid-washed 500-ml polycarbonate incubation bottles to which red rubber septa had been attached with silicone sealant. The sealant had been aged to assure complete curing, and the bottles were incubated upright to prevent contact between the sample and the septum and sealant. We used gas chromatography with flame ionization detection (Hardy et al. 1973) to determine that $<10\%$ of the C_2H_2 in the headspace diffused through the polycarbonate container over the duration of a typical incubation.

From each depth, two to four replicate incubation bottles were filled for controls and an equal number were filled for the C_2H_2 treatments. Each bottle was inoculated with 2.8–7.4 MBq of $H^{14}CO_3^-$ and then quickly treated with the inhibitor. Acetylene (3 ml) was injected into the headspace through the septum with a syringe after an equal volume of air had been removed. In this protocol, the final C_2H_2 concentration calculated to exist in the aqueous phase (Flett et al. 1976) was always more than an order of magnitude greater than the 3.8 μM required for complete inhibition of ammonium oxidation in pure cultures of the ammonium oxidizing bacterium *Nitrosomonas europaea* (Hynes and Knowles 1981). The incubation bottles were gently agitated to evenly distribute the radiocarbon and the inhibitor, covered with opaque bags, and placed in temperature-controlled water baths for $\sim$24 h. The in situ temperatures were matched to ± 1°C. After the incubations, the samples were vacuum-filtered through 0.2-μm polycarbonate membrane filters (Nuclepore). The ^{14}C activity was determined by means of liquid scintillation counting as described by Letelier et al. (1996). Dissolved inorganic carbon concentrations (used to calculate carbon assimilation rates) were determined independently by CO_2 coulometry (Winn et al. 1994).

Because the ^{14}C-based assay measures carbon incorporation as a surrogate for ammonium oxidation, a conversion factor must be applied to obtain the latter rate from the former. Several studies have reported such factors for marine nitrifiers, ranging from 8.3 to 42 mol NH_4^+ oxidized per mol C fixed during ammonium oxidation (Carlucci and Strickland 1968; Billen 1976; Glover 1985). This large range probably reflects both a lack of obligate coupling between the oxidation of ammonium and carbon fixation in nitrifying bacteria and a varied response of nitrifiers to different environmental parameters. We have adopted the lower value of 8.3 (Billen 1976) because of the observation by Feliatra and Bianchi (1993) that nitrifiers in seawater generally have the lowest N : C when compared to nitrifiers in other natural aquatic environments. The empirical N : C measured independently by combining our data from the ^{14}C experiments and the chemical assay (*see below*) suggest that this was a reasonable, yet perhaps somewhat low, conversion factor.

The second method used to assess nitrification rates involves direct measurement of the changes in NO_2^- and NO_3^- in incubated samples. Replicate samples were incubated in the dark in 500-ml acid-washed polycarbonate bottles without any additions for $\sim$24 h. Ammonium oxidation was determined by the change of the total N+N over the course of the incubation, and nitrite oxidation by the change in NO_3^- alone. Although processes other than nitrification may alter concentrations of NO_3^- and NO_2^-, even in total darkness (e.g. phytoplankton nitrate reduction), nitrification is expected to dominate the conversions of these nitrogen species in the absence of light energy. Heterotrophic nitrification, although it has not been conclusively demonstrated to occur in seawater (Kaplan 1983), would be included by the chemical measurements. However, because heterotrophic nitrification is not an autotrophic process, it would have less effect on the ^{14}C-based measurements and would also cause the two independent estimates of nitrification to diverge.

The above assays both involve 24-h dark incubations with single-endpoint determinations. Although time-course experiments were not performed, the single-endpoint measurements are justified by observations of linearity in ammonium oxidation rates over 24 h in previous time-course experiments (Olson 1981*a*). We used dark incubations in both of the above assays to avoid interference from phytoplankton nitrate assimilation and carbon incorporation that would swamp the nitrifier signal in light incubations. However, it is possible that nitrifying bacteria may show some recovery from photoinhibition over the course of a 24-h incubation. In laboratory studies with pure nitrifier cultures, ammonium oxidizers recovered 35% of their activity and nitrite oxidizers recovered 3% 24 h after exposure to sunlight (Vanzella et al. 1990). Olson (1981*a*) made simultaneous 24-h light and dark measurements of ammonium oxidation on two samples from the PNM in the North Pacific subtropical gyre with ^{15}N tracer methodology and found that the light incu-

Table 1. Nitrification rates at Station ALOHA estimated with an inhibitor-sensitive radiocarbon uptake assay (^{14}C) and a chemical assay (Chem). Values presented are means ±1 SE, calculated by propagation of the errors in control and treatment groups (not determined—nd).

Cruise and date	Depth (m)	Method	Oxidation rate (μmol m^{-3} d^{-1}) NH_4^+	NO_2^-
HOT-31	131	^{14}C	9.8±5.5	nd
Oct 91		Chem	32.3±24.9	9.6±17.8
	152	^{14}C	122.6±15.5	nd
		Chem	137.4±109.6	138.0±124.4
HOT-36	140	^{14}C	1.0±3.8	nd
Apr 92	164	^{14}C	21.8±11.8	nd
	172	^{14}C	80.2±60.2	nd
HOT-50	106	Chem	1.4±0.2	−0.2±0.2
Oct 93	135	Chem	6.8±1.6	2.8±1.6
	155	Chem	23.3±4.0	18.6±3.8
	175	Chem	10.5±5.5	8.8±5.8

bations yielded rates 70 and 96% of those from the respective dark incubations. Recovery from light inhibition thus may potentially introduce overestimates of ammonium oxidation rate of up to 43%, but should have little effect on the nitrite oxidation measurements.

On one cruise (HOT-50), we performed an in situ incubation and used the chemiluminescent method to measure changes in nitrite and nitrate in the incubated samples. On an early morning rosette cast, we collected water-column samples at 10-m intervals throughout the euphotic zone. From each of these, a single 250-ml acid-washed clear polycarbonate incubation bottle was filled and tightly capped under subdued light. Replicate samples were immediately frozen in 125-ml polyethylene bottles for time-zero analyses. Before dawn, the incubation bottles were attached to the HOT free-floating sediment trap array at the depths from which they were collected. The deployment lasted 72 h. After recovery, the incubation bottles were immediately frozen and returned along with the time-zero samples to our shore-based laboratory for chemiluminescent nitrate and nitrite analyses. Although the long duration of this deployment could possibly have resulted in artifacts (Venrick et al. 1977), we needed to capture at least one full diel cycle to determine net daily rates, and the 72-h sediment trap deployment was a convenient vehicle for doing so. Nonlinearity of rate processes over the course of the incubation is possible, so the results should be interpreted with some caution.

Results and discussion

Nitrification rates—Nitrification rates in the lower euphotic zone (100–175 m) were highly variable with depth and between cruises (Table 1). Ammonium oxidation rates were sometimes substantial, reaching a maximum of 137.4 μmol m^{-3} d^{-1} (mean, 40.6 μmol m^{-3} d^{-1}; median, 21.8 μmol m^{-3} d^{-1}; n = 11). Nitrite oxidation rates were comparable, with a maximum of 138.0 μmol m^{-3} d^{-1} (mean, 29.6 μmol m^{-3} d^{-1}; median, 9.2 μmol m^{-3} d^{-1}; n = 6). Although ammonium oxidation exceeded nitrite oxidation in five of six cases, the high variability associated with each measurement makes these differences statistically insignificant; also, because the ammonium oxidation rates are potentially overestimated by up to 43% owing to recovery from photoinhibition, the ammonium and nitrite oxidation rates may tend to converge. The two independent methods used to assess ammonium oxidation rates on HOT-31, although exhibiting a high degree of variability, agreed reasonably well, but suggest that the N:C conversion factor used may have been somewhat low.

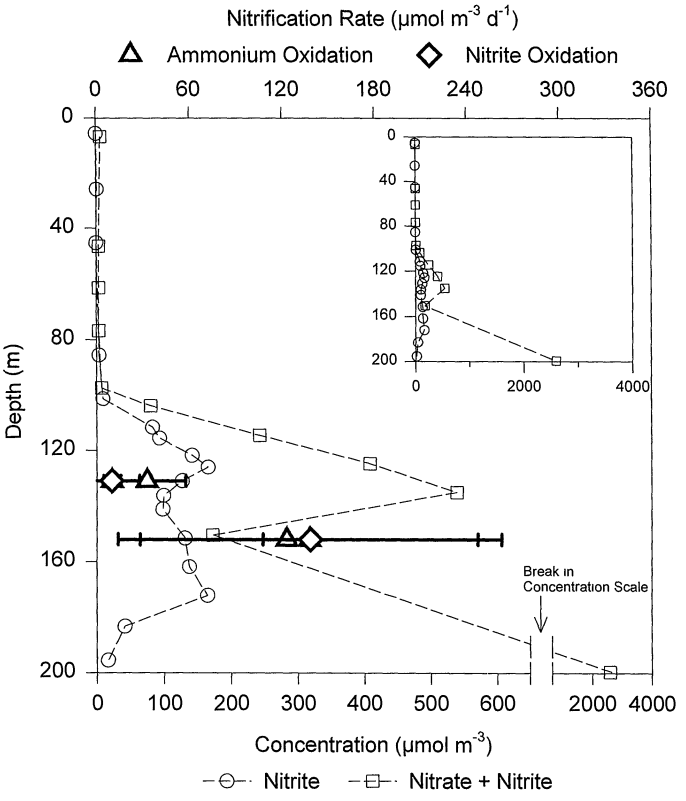


Fig. 1. Depth profiles of selected nitrogen cycle parameters at Station ALOHA during HOT-31. Nitrite and nitrate+nitrite were measured by chemiluminescence, ammonium oxidation rates were estimated with both the ^{14}C and chemical methods (*see text*), and nitrite oxidation rates were estimated with the chemical method. Error bars are ±1 SE, calculated by propagating the SEs between control or time-zero and incubated groups of two to four samples each. Inset shows nitrite and nitrate+nitrite concentrations without break in scale in order to emphasize relative pool sizes.

There are few previous measurements of nitrification rates in the lower euphotic zone of the North Pacific subtropical gyre. Measurements of ammonium oxidation rates in the PNM by ^{15}N tracer methodology made at 30°N, 155°W ranged from 2.2 to 7.3 μmol m^{-3} d^{-1} and averaged 4.3 (Olson 1981*a*). This entire data set was from a single cruise over a period of 2 weeks, and no more

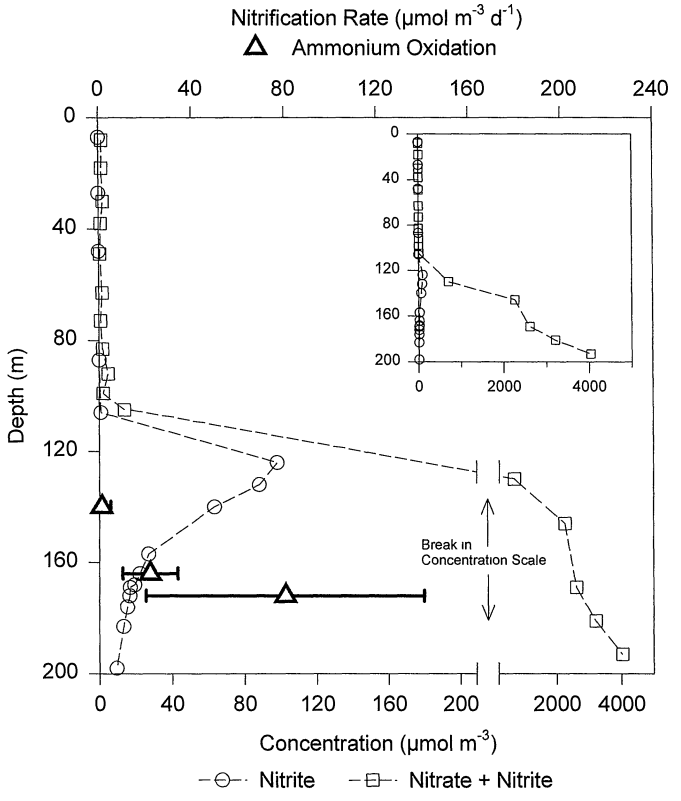


Fig. 2. Depth profiles of selected nitrogen cycle parameters at Station ALOHA during HOT-36. Details as in Fig. 1, except that only ^{14}C-based ammonium oxidation rates were estimated and nitrite oxidation rates were not determined.

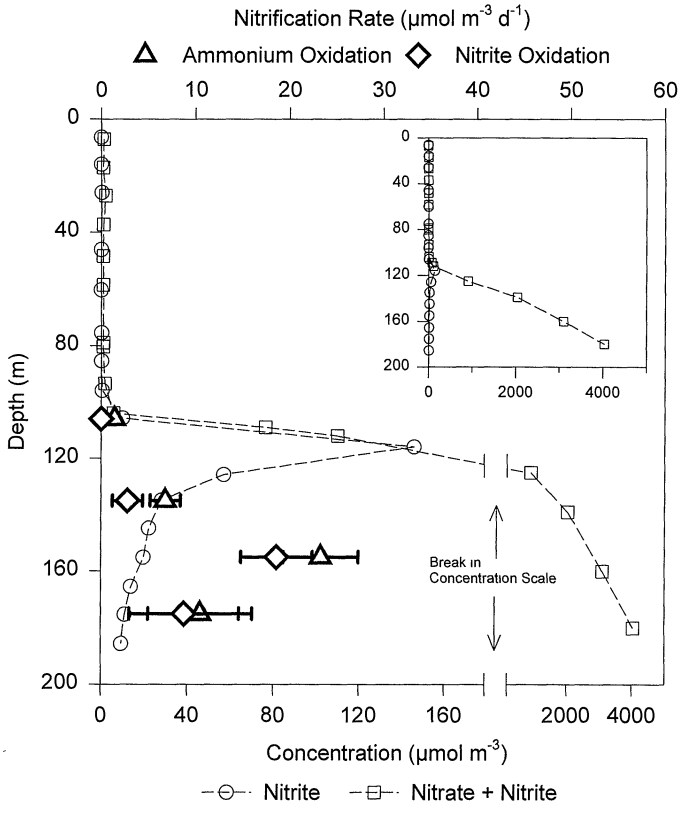


Fig. 3. Depth profiles of selected nitrogen cycle parameters at Station ALOHA during HOT-50. Details as in Fig. 1, except that only chemical-based ammonium oxidation rates and nitrite oxidation rates were determined.

than one depth was sampled on any given day. It is therefore difficult to directly compare the variability in nitrification rates with depth and time between the two data sets. However, note that the highest rates observed at Station ALOHA on each cruise were found below 150 m, whereas the deepest sample assayed by Olson (1981*a*) was from 148 m; above 150 m the two data sets exhibit a fair degree of similarity. Nitrification rates of >200 μmol m^{-3} d^{-1} have been measured or estimated in other, less oligotrophic marine environments (Ward 1982; Priscu and Downes 1985; Feliatra and Bianchi 1993), whereas the farthest offshore stations examined in nitrification studies of the Southern California Bight (Olson 1981*a*) and off the coast of Washington (Ward et al. 1984) exhibited ammonium oxidation rates in the PNM of up to 20 μmol m^{-3} d^{-1}. We think that we are converging on lower euphotic zone nitrification rates representative of the central gyre habitat.

If we use the mean values from our measurements above and assume they are typical of the 100–175-m layer, while also assuming nitrification is absent in the 0–100-m layer owing to photoinhibition, we arrive at total euphotic zone nitrification rates of 3.05 and 2.22 mmol m^{-2} d^{-1} for ammonium and nitrite oxidation, respectively. Because the data set is small and not distributed normally, more conservative estimates based on median rates may be in order. Such conservative rates would be 1.64 and 0.69 mmol m^{-2} d^{-1} for ammonium and nitrite oxidation.

Nitrification and the primary nitrite maximum—Water-column profiles of NO_2^- and N+N from the three HOT cruises discussed here show a primary nitrite maximum that begins a few meters beneath the top of the nitrate gradient or nitracline (Figs. 1–3). During HOT-31, an inversion in the N+N profile is evident at ~150 m (Fig. 1). Nevertheless, during each of these cruises, both ammonium oxidation rates and (where available) nitrite oxidation rates within the large upper peak of the primary nitrite maximum are lower than they are a few meters below, within the "tail" of the nitrite distribution (Figs. 1–3). This finding is consistent with our earlier hypothesis that this upper PNM (UPNM) is maintained by algal reduction of nitrate rather than by bacterial ammonium oxidation, whereas ammonium oxidation contributes a larger share of the nitrite below this feature (Dore and Karl 1996).

The results of the HOT-50 in situ incubation reveal substantial net uptake of N+N within the UPNM (100–140 m)—up to 17.9 μmol m^{-3} d^{-1} (Fig. 4). A zone of net N+N production is seen below the UPNM, from 150 to 160 m, with maximum rates of 5.9 μmol m^{-3} d^{-1}. This layer of net N+N production is coincident with the maximum ammonium oxidation rates from the HOT-50 dark

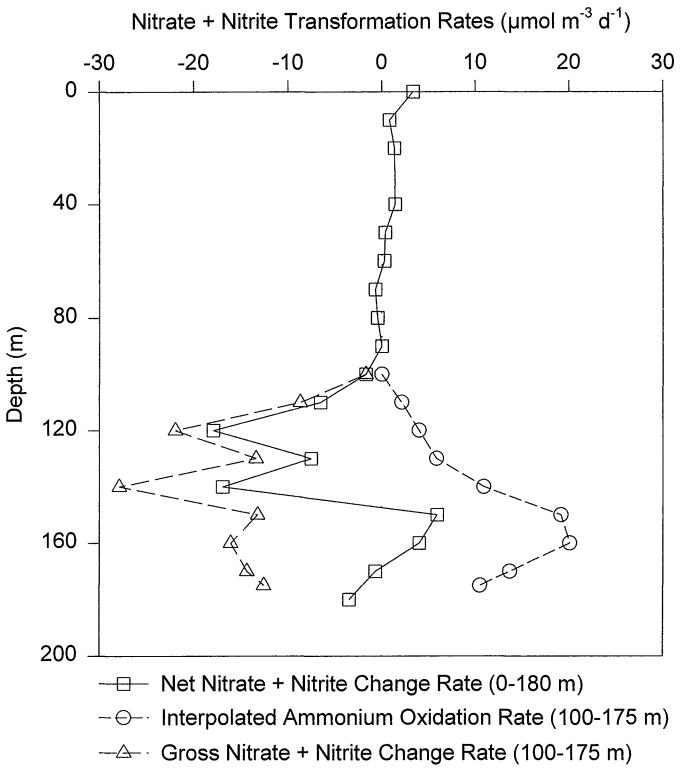


Fig. 4. Depth profiles of measured and estimated nitrate+nitrite transformation rates from HOT-50. Net rates of change in nitrate+nitrite during a 3-d in situ incubation—□. Ammonium oxidation rates interpolated from the dark incubation data presented in Fig. 1 and Table 1—○. Gross nitrate+nitrite uptake rates calculated by subtraction of interpolated ammonium oxidation rates from net nitrate+nitrite uptake rates—△. Dotted line indicates zero rate of change.

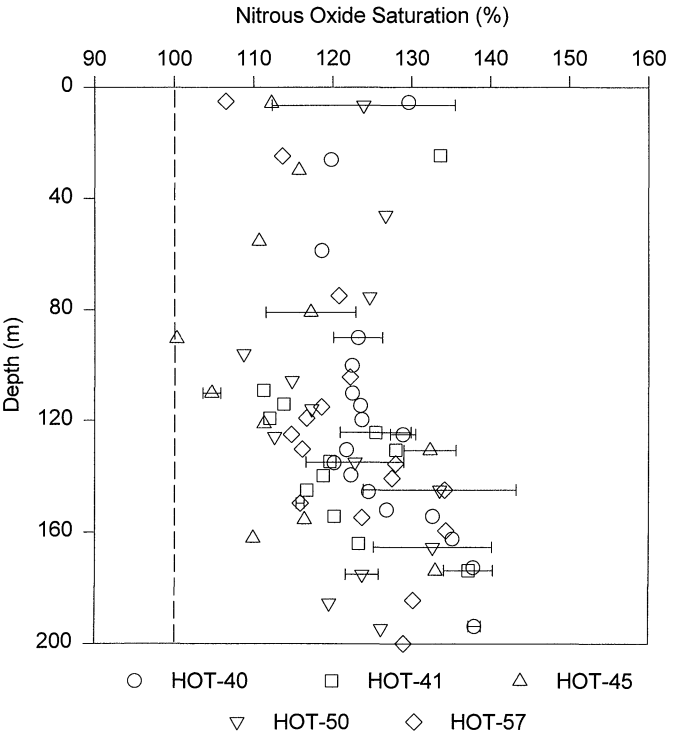


Fig. 5. Depth distributions of nitrous oxide expressed as a percentage of air saturation values. Error bars are ±1 SE of replicate measurements. Dashed line indicates equilibrium with atmospheric nitrous oxide at in situ temperature and salinity.

incubation (Figs. 3, 4). The results of this in situ incubation, like those of the dark incubation, are consistent with a vertical separation of oxidative and reductive nitrite sources, reduction of nitrate dominating within the UPNM, and oxidation of ammonium becoming more important below.

Nitrification and N_2O—Nitrous oxide exhibited supersaturation throughout the euphotic zone at Station ALOHA (Fig. 5). The concentration of N_2O in the surface mixed layer varied from 6.7 to 8.3 μmol m^{-3} (107–134% of air saturation), with a five-cruise mean of 7.6 μmol m^{-3} (121% saturation). At the base of the euphotic zone (175 m), N_2O ranged from 8.3 to 10.5 μmol m^{-3} (120–138% saturation) and increased along a concentration gradient into deeper waters. The small headspace in the sample bottles (~5 ml) was considered essential for long-term storage, but unfortunately may have introduced a slight but variable underestimate of N_2O in these samples; we calculate that this error is no more than 0.6% for the most supersaturated samples. A paucity of published data on N_2O distributions in the North Pacific subtropical gyre limits the potential for direct comparison of our data with those of other investigators. However, the 0–200-m depth distribution of N_2O observed in our study (Fig. 5) is similar to that measured by Elkins et al. (1978) at 20°N, 150°W. These investigators reported a surface saturation of ~125%, while Singh et al. (1979) reported ~130% saturation during a north–south transect across the Pacific as they passed by 20°N at ~135°W. Nevison et al. (1995) also reported N_2O supersaturation near Station ALOHA, but of lower magnitude (~103% saturation).

We can use our information on N_2O distributions to derive an independent estimate of nitrification rates in the euphotic zone at Station ALOHA. If we assume steady-state conditions and no horizontal advection of N_2O, the flux of N_2O to the atmosphere from the supersaturated surface waters must be balanced by the vertical eddy-diffusive flux from deeper waters plus in situ N_2O production. A negative correlation of N_2O and dissolved oxygen in the water column is a common feature of much of the ocean worldwide and is indicative of N_2O production via nitrification (Elkins et al. 1978; Cohen and Gordon 1979; Oudot et al. 1990). Chemoautotrophic ammonium oxidation produces nitrous oxide as a by-product, and the relative yield of N_2O with respect to NO_2^- varies inversely with the dissolved oxygen concentration (Goreau et al. 1980; Lipschultz et al. 1981). In the well-oxygenated waters of the euphotic zone at Station ALOHA, the primary if not the sole in situ source of N_2O is expected to be ammonium oxidation.

We can estimate the sea-air flux of nitrous oxide based on an empirically derived relationship between gas transfer and wind speed (Wanninkhof 1992) by using our mea-

Table 2. Euphotic zone (0–175 m) nitrous oxide budget at station ALOHA. Sea-air fluxes (μmol m^{-2} d^{-1}) are calculated from sea surface temperature (°C), mean wind speed (m s^{-1}), and mean mixed layer ΔN_2O (=$N_2O_{meas.}$ − $N_2O_{air\ sat}$) (μmol m^{-3}) with the equations of Wanninkhof (1992). Vertical N_2O fluxes (μmol m^{-2} d^{-1}) are calculated from the measured N_2O concentration gradient (μmol m^{-4}) at 175 m with an eddy diffusion coefficient of 3.7×10^{-5} m^2 s^{-1} (Lewis et al. 1986). The 0–175-m production rate of N_2O (μmol m^{-2} d^{-1}) is estimated as the difference between the sea-air flux and the vertical diffusive flux. NH_4^+ oxidation rate (mmol m^{-2} d^{-1}) is estimated based on the 0–175-m N_2O production rate and a molar yield of 0.5% for N_2O relative to NH_4^+ oxidized (*see text*).

				N_2O				
Cruise	Mixed layer ΔN_2O	Sea surface temp	Mean wind speed	Sea-air flux	Vertical gradient	Vertical flux	Prod. rate	NH_4^+ oxidation rate
HOT-40								
Sep 92	1.55	26.4	6.83	6.07	0.027	0.09	5.98	1.20
HOT-41								
Oct 92	2.10	26.5	4.16	3.06	0.051	0.16	2.90	0.58
HOT-45								
Feb 93	0.82	23.8	5.32	1.83	0.049	0.16	1.68	0.34
HOT-50								
Oct 93	1.53	25.5	8.04	8.11	0.054	0.17	7.94	1.59
HOT-57								
Sep 94	0.63	26.5	7.02	2.61	0.028	0.09	2.52	0.50

surements of surface ΔN_2O (= N_2O_{meas} − $N_2O_{air\ sat}$), temperature, and wind speed (Table 2). This model takes into account the effects of wind speed variability and the solubility of the gas in seawater. When calculated in this way, we arrive at a sea-air N_2O flux of 1.83–8.11 μmol m^{-2} d^{-1} for the five cruises considered (Table 2). We can simultaneously estimate the vertical N_2O flux from below the euphotic zone by means of a one-dimensional eddy-diffusive model, in which the flux equals the product of the concentration gradient and an eddy-diffusivity coefficient. From our N_2O profiles, we determine that the vertical N_2O concentration gradient at 175 m is 0.027–0.054 μmol m^{-4}. We use an eddy-diffusivity coefficient of 3.7×10^{-5} m^2 s^{-1} (Lewis et al. 1986) and calculate a vertical N_2O flux of 0.09–0.17 μmol m^{-2} d^{-1} (Table 2). The difference between the sea-air flux and the vertical eddy-diffusive flux is a net euphotic zone N_2O production rate of 1.68–7.94 μmol m^{-2} d^{-1}.

We then assume that N_2O is produced at a rate that is 0.5% of the ammonium oxidation rate. Under well-oxygenated conditions, this yield has been shown to vary from <0.1% to ~0.5% (Goreau et al. 1980; Lipschultz et al. 1981; Kaplan and Wofsy 1985). We choose here to use the highest yield because it results in the most conservative estimate of nitrification rate. The resulting estimates of ammonium oxidation rate in the euphotic zone are 0.34–1.59 mmol m^{-2} d^{-1}.

These calculations reveal that the euphotic zone production of N_2O by nitrifying bacteria may exceed the vertical flux into this layer from below by a factor of 18–66. We recognize that these calculations depend heavily on the choice of eddy-diffusivity coefficient and on the ratio of N_2O to NO_2^- produced during ammonium oxidation. Also, the variability of our measurements of the mixed-layer N_2O saturation state reduces the precision of our sea-air N_2O flux estimates. Nevertheless, these results strongly suggest that much of the dissolved N_2O that could be released to the atmosphere at Station ALOHA is produced within the euphotic zone. The results also provide an independent conservative estimate of the overall euphotic zone ammonium oxidation rate that is on the same order as that from the incubation results above. Interestingly, the saturation state of N_2O in the upper 40 m seems to be equal to or slightly higher than that immediately below 40 m (Fig. 5); this could indicate near-surface nitrification despite the inhibitory effect of light on nitrifying bacteria.

Nitrification and new production—When the new production concept was developed by Dugdale and Goering (1967), accurate measurements of marine nitrification rates were not available. Nevertheless, Dugdale and Goering were aware that nitrification could prove to be a bane to their model. They stated, "If nitrification rates are eventually shown to be sufficiently higher than has been assumed, the assumption that nitrate is a nonregenerated nutrient form in the euphotic zone would have to be modified" (Dugdale and Goering 1967, p. 205). More recently, the new production concept has been extended to equate nitrate-based production with export production to determine the fraction of carbon that can be removed from the euphotic zone by the "biological pump" (Eppley and Peterson 1979; Longhurst and Harrison 1989). However, because improvements in techniques for the measurement of nitrification rates in the sea indicate a significant role for this process (Olson 1981*a*; Ward et al. 1982), the validity of the new production concept as it is commonly applied has come into question (Priscu and Downes 1985; Ward et al. 1989). It is therefore of great interest to compare nitrification rates with nitrate uptake rates and the eddy-diffusive supply of nitrate to the euphotic zone.

We focus here on the experiments conducted during HOT-50, from which we have the most complete data set; however, we recognize that higher nitrification rates were measured during HOT-31 and HOT-36. The HOT-50 in situ incubation provides us with an estimate of 0.36 mmol m^{-2} d^{-1} for euphotic zone depth-integrated net N+N uptake (Fig. 4, Table 3). However, to obtain an estimate of the gross N+N uptake, we must add the rate of ammonium oxidation to this net figure. To facilitate this calculation, we use a linear interpolation of the ammonium oxidation data from the dark incubation between 100 and 175 m and assume zero nitrification from the surface to 100 m (Fig. 4). The resulting profile of gross N+N uptake yields an integrated (100–175 m) rate of 1.12 mmol m^{-2} d^{-1} (Table 3). This estimate is well within the range of previous measurements of gross N+N uptake, based on ^{15}N tracer methodology, that have been made in the North Pacific subtropical gyre (0.23–1.67

Table 3. Estimates of euphotic zone nitrification rates and nitrate uptake rates from HOT-50 compared with those from previous studies in the North Pacific subtropical gyre.

Type of estimate	Source and site	Rate (mmol m^{-2} d^{-1})
Nitrification rates		
Ammonium oxidation based on change in nitrate+nitrite during dark incubations; 100–175 m integrated	HOT-50 Station ALOHA	0.76
Nitrite oxidation based on change in nitrate during dark incubations; 100–175 m integrated	HOT-50 Station ALOHA	0.53
Ammonium oxidation based on N_2O budget calculations (0–175 m) and a 0.5% N_2O yield	HOT-50 Station ALOHA	1.59
Ammonium oxidation based on mean of five ^{15}N tracer measurements over 100–175-m depth range	Olson 1981*a* 30°N, 155°W	0.32
Nitrate uptake rates		
Net nitrate+nitrite uptake based on concentration change during in situ incubation; 0–180 m	HOT-50 Station ALOHA	0.36
Gross nitrate+nitrite uptake based on concentration change during in situ incubation combined with dark ammonium oxidation measurements; 100–175 m	HOT-50 Station ALOHA	1.12
Vertical eddy-diffusive flux of nitrate+nitrite based on measured gradient and a diffusion coefficient of 3.7×10^{-5} m^2 s^{-1}	HOT-50 Station ALOHA	0.17
Uptake of nitrate based on ^{15}N tracer measurements; 0–90 m integrated	Sahlsten 1987 28°N, 155°W	1.67
Uptake of nitrate based on ^{15}N tracer measurements; 0–160 m integrated, range from six cruises	Knauer et al. 1990 33°N, 139°W	0.23–0.79

mmol m^{-2} d^{-1}, Table 3). The eddy-diffusive flux of N+N into the euphotic zone during HOT-50 is estimated to have been 0.17 mmol m^{-2} d^{-1} based on the measured gradient and an eddy-diffusion coefficient of 3.7×10^{-5} m^2 s^{-1} (Lewis et al. 1986). This flux represents about half of the net N+N uptake but only 15% of the gross N+N uptake estimated above (Table 3). Interestingly, the HOT-50 in situ incubation reveals a slight net production of N+N in the upper 40 m of the water column (Fig. 4). This observation may indicate that nitrification is not fully inhibited by light in the upper 100 m and is consistent with the elevated N_2O saturations in the upper 40 m (Fig. 5). Nevertheless, because we do not have independent nitrification rate measurements in this upper layer, we will continue to make the conservative assumption in our depth-integrated calculations that nitrification in the upper 100 m is nil.

Integrated (100–175 m) nitrification rates from the dark incubation during HOT-50 were 0.53 mmol m^{-2} d^{-1} for nitrite oxidation and 0.76 mmol m^{-2} d^{-1} for ammonium oxidation (Table 3). At the same time, the 0–175-m integrated ammonium oxidation rate estimated from the N_2O budget was 1.59 mmol m^{-2} d^{-1}. An historical estimate of 0.32 mmol m^{-2} d^{-1} comes from averaging the ammonium oxidation data of Olson (1981*a*) and assuming that the value holds over the 100–175-m depth range (Table 3). Because Olson's data do not include points from the 150–175-m depth range (where we find the highest ammonium oxidation rates), this estimate is likely to be low.

We find that for the HOT-50 experiments nitrification represents between 47 and 142% of the contemporaneous gross N+N assimilation rate (Table 3). Although the historical estimates of nitrification and nitrate uptake rates in the North Pacific subtropical gyre come from different sources and locations, they suggest a range of 19–139% for this ratio, which is consistent with our findings. Given the uncertainties in our own data, the uncertainties presented by previous investigators, the small size of the combined data set, and the high degree of variability with depth and time, it is difficult to present a robust estimate of the relative overall magnitudes of the nitrification and nitrate assimilation processes for the North Pacific subtropical gyre. However, we are beginning to see a convergence of estimates that indicates that the two processes have rates on the same order of magnitude and that suggests that a substantial fraction of nitrate assimilated is regenerated and not new. Similar conclusions have been reached for the western Cook Strait, New Zealand (Priscu and Downes 1985), and for the Southern California Bight (Ward et al. 1989). If Station ALOHA is representative of oligotrophic oceanic gyre habitats in general, then the use of measurements of gross nitrate assimilation rates to estimate new production is precluded over vast areas of the world's oceans, unless concurrent nitrification rate measurements are included.

References

BILLEN, G. 1976. Evaluation of nitrifying activity in sediments by dark C-14 bicarbonate incorporation. Water Res. **10:** 51–57.

BINGHAM, F., AND R. LUKAS. 1996. Seasonal cycles of temperature, salinity and dissolved oxygen observed in the Hawaii Ocean Time-series. Deep-Sea Res. Part 2 **43:** 199–213.

BRANDHORST, W. 1959. Nitrification and denitrification in the eastern tropical North Pacific. J. Cons. Cons. Int. Explor. Mer **25:** 2–20.

BUTLER, J. H., AND J. W. ELKINS. 1991. An automated technique for the measurement of dissolved N_2O in natural waters. Mar. Chem. **34:** 47–61.

CAPONE, D. G. 1991. Aspects of the marine nitrogen cycle with relevance to the dynamics of nitrous and nitric oxide, p. 255–275. *In* J. E. Rogers and W. B. Whitman [eds.], Microbial production and consumption of greenhouse gases: Methane, nitrogen oxides, and halomethanes. Am. Soc. Microbiol.

CARLUCCI, A. F., AND J. D. H. STRICKLAND. 1968. The isolation, purification and some kinetic studies of marine nitrifying bacteria. J. Exp. Mar. Biol. Ecol. **2:** 156–166.

COHEN, Y., AND L. I. GORDON. 1979. Nitrous oxide production in the ocean. J. Geophys. Res. **84:** 347–353.

COX, R. D. 1980. Determination of nitrate and nitrite at the parts per billion level by chemiluminescence. Anal. Chem. **52:** 332–335.

DORE, J. E., AND OTHERS. 1996. Freezing as a method of sample preservation for the analysis of dissolved inorganic nutrients in seawater. Mar. Chem. **53:** 173–185.

———, AND D. M. KARL. 1996. Nitrite distributions and dynamics at Station ALOHA. Deep-Sea Res. Part 2 **43:** 385–402.

DUGDALE, R. C., AND J. J. GOERING. 1967. Uptake of new and regenerated forms of nitrogen in primary productivity. Limnol. Oceanogr. **12:** 196–206.

ELKINS, J. W. 1980. Determination of dissolved nitrous oxide in aquatic systems by gas chromatography using electron-capture detection and multiple phase equilibration. Anal. Chem. **52:** 263–267.

———, S. C. WOFSY, M. B. MCELROY, C. E. KOLB, AND W. A. KAPLAN. 1978. Aquatic sources and sinks for nitrous oxide. Nature **275:** 602–606.

EPPLEY, R. W., AND B. J. PETERSON. 1979. Particulate organic matter flux and planktonic new production in the deep ocean. Nature **282:** 677–680.

FELIATRA, F., AND M. BIANCHI. 1993. Rates of nitrification and carbon uptake in the Rhône River plume (northwestern Mediterranean Sea). Microb. Ecol. **26:** 21–28.

FLETT, R. J., R. D. HAMILTON, AND N. E. R. CAMPBELL. 1976. Aquatic acetylene-reduction techniques: Solutions to several problems. Can. J. Microbiol. **22:** 43–51.

GARSIDE, C. 1982. A chemiluminescent technique for the determination of nanomolar concentrations of nitrate and nitrite in seawater. Mar. Chem. **11:** 159–167.

GLOVER, H. E. 1985. The relationship between inorganic nitrogen oxidation and organic carbon production in batch and chemostat cultures of marine nitrifying bacteria. Arch. Microbiol. **74:** 295–300.

GOREAU, T. J., AND OTHERS. 1980. Production of NO_2^- and N_2O by nitrifying bacteria at reduced concentrations of oxygen. Appl. Environ. Microbiol. **40:** 526–532.

HARDY, R. W. F., R. C. BURNS, AND R. D. HOLSTEN. 1973. Applications of the acetylene-ethylene assay for measurement of nitrogen fixation. Soil Biol. Biochem. **5:** 47–81.

HERBLAND, A., AND B. VOITURIEZ. 1979. Hydrological structure analysis for estimating the primary production in the tropical Atlantic Ocean. J. Mar. Res. **37:** 87–101.

HOUGHTON, J. T., G. J. JENKINS, AND J. J. EPHRAUMS [EDS.]. 1990. Climate change: The IPCC scientific assessment. Cambridge.

HYNES, R. K., AND R. KNOWLES. 1981. Effect of acetylene on autotrophic and heterotrophic nitrification. Can. J. Microbiol. **28:** 334–340.

KAPLAN, W. A. 1983. Nitrification, p. 139–190. *In* E. J. Carpenter and D. G. Capone [eds.], Nitrogen in the marine environment. Academic.

———, AND S. C. WOFSY. 1985. The biogeochemistry of nitrous oxide: A review, p. 181–206. *In* H. W. Jannasch and P. J. leB. Williams [eds.], Advances in aquatic microbiology. V. 3. Academic.

KARL, D. M., AND R. LUKAS. 1996. The Hawaii Ocean Time-series (HOT) program: Background, rationale and field implementation. Deep-Sea Res. Part 2 **43:** 129–156.

KIEFER, D. A., R. J. OLSON, AND O. HOLM-HANSEN. 1976. Another look at the nitrite and chlorophyll maxima in the central North Pacific. Deep-Sea Res. **23:** 1199–1208.

KNAUER, G. A., D. G. REDALJE, W. G. HARRISON, AND D. M. KARL. 1990. New production at the VERTEX time-series site. Deep-Sea Res. **37:** 1121–1134.

LETELIER, R. M., J. E. DORE, C. D. WINN, AND D. M. KARL. 1996. Seasonal and interannual variations in photosynthetic carbon assimilation at Station ALOHA. Deep-Sea Res. Part 2 **43:** 467–490.

LEWIS, M. R., W. G. HARRISON, N. S. OAKEY, D. HEBERT, AND T. PLATT. 1986. Vertical nitrate fluxes in the oligotrophic ocean. Science **234:** 870–873.

LIPSCHULTZ, F., AND OTHERS. 1981. Production of NO and N_2O by soil nitrifying bacteria. Nature **294:** 641–643.

LONGHURST, A. R., AND W. G. HARRISON. 1989. The biological pump: Profiles of plankton production and consumption in the upper ocean. Prog. Oceanogr. **22:** 47–123.

NEVISON, C. D., R. F. WEISS, AND D. J. ERICKSON III. 1995. Global oceanic emissions of nitrous oxide. J. Geophys. Res. **100:** 15,809–15,820.

OLSON, R. J. 1981*a*. ^{15}N tracer studies of the primary nitrite maximum. J. Mar. Res. **39:** 203–226.

———. 1981*b*. Differential photoinhibition of marine nitrifying bacteria: A possible mechanism for the formation of the primary nitrite maximum. J. Mar. Res. **39:** 227–238.

OUDOT, C., C. ANDRIE, AND Y. MONTEL. 1990. Nitrous oxide production in the tropical Atlantic Ocean. Deep-Sea Res. **37:** 183–202.

PRISCU, J. C., AND M. T. DOWNES. 1985. Nitrogen uptake, ammonium oxidation and nitrous oxide (N_2O) levels in the coastal waters of western Cook Strait, New Zealand. Estuarine Coastal Shelf Sci. **20:** 529–542.

RAKESTRAW, N. W. 1936. The occurrence and significance of nitrite in the sea. Biol. Bull. **71:** 133–167.

RASMUSSEN, R. A., AND D. PIEROTTI. 1978. Interlaboratory calibration of atmospheric nitrous oxide measurements. Geophys. Res. Lett. **5:** 353–355.

RITCHIE, G. A. F., AND D. J. D. NICHOLAS. 1972. Identification of the sources of nitrous oxide produced by oxidative and reductive processes in *Nitrosomonas europaea*. Biochem. J. **126:** 1181–1191.

SAHLSTEN, E. 1987. Nitrogenous nutrition in the euphotic zone of the central North Pacific Gyre. Mar. Biol. **96:** 433–439.

SINGH, H. B., L. J. SALAS, AND H. SHIGEISHI. 1979. The distribution of nitrous oxide (N_2O) in the global atmosphere and the Pacific Ocean. Tellus **31:** 313–320.

SOMVILLE, M. 1978. A method for the measurement of nitrification rates in water. Water Res. **12:** 843–848.

SVERDRUP, H. U. 1953. On conditions for the vernal blooming of phytoplankton. J. Cons. Cons. Int. Explor. Mer **18:** 287–295.

VACCARO, R. F., AND J. H. RYTHER. 1960. Marine phytoplankton and the distribution of nitrite in the sea. J. Cons. Cons Int. Explor. Mer **25:** 260–271.

VANZELLA, A., M. A. GUERRERO, AND R. D. JONES. 1990. Recovery of nitrification in marine bacteria following exposure

to carbon monoxide or light. Mar. Ecol. Prog. Ser. **60:** 91–95.

VENRICK, E. L., J. R. BEERS, AND J. F. HEINBOKEL. 1977. Possible consequences of containing microplankton for physiological rate measurements. J. Exp. Mar. Biol. Ecol. **26:** 55–76.

WANNINKHOF, R. 1992. Relationship between wind speed and gas exchange over the ocean. J. Geophys. Res. **97:** 7373–7382.

WARD, B. B. 1982. Oceanic distribution of ammonium-oxidizing bacteria determined by immunofluorescent assay. J. Mar. Res. **40:** 1155–1172.

———. 1986. Nitrification in marine environments, p. 157–184. *In* J. I. Prosser [ed.], Nitrification. IRL.

———, K. A. KILPATRICK, E. H. RENGER, AND R. W. EPPLEY. 1989. Biological nitrogen cycling in the nitracline. Limnol. Oceanogr. **34:** 493–513.

———, R. J. OLSON, AND M. J. PERRY. 1982. Microbial nitrification rates in the primary nitrite maximum off southern California. Deep-Sea Res. **29:** 247–255.

———, M. C. TALBOT, AND M. J. PERRY. 1984. Contributions of phytoplankton and nitrifying bacteria to ammonium and nitrite dynamics in coastal waters. Cont. Shelf Res. **3:** 383–398.

WEISS, R. F., AND B. A. PRICE. 1980. Nitrous oxide solubility in water and seawater. Mar. Chem. **8:** 347–359.

WINN, C. D., F. T. MACKENZIE, C. J. CARRILLO, C. L. SABINE, AND D. M. KARL. 1994. Air-sea carbon dioxide exchange in the North Pacific subtropical gyre: Implications for the global carbon budget. Global Biogeochem. Cycles **8:** 157–163.

Submitted: 22 May 1995
Accepted: 27 March 1996
Amended: 24 July 1996